

Further Evaluation of an Elevated Mixed-Layer Model for Altocumulus Clouds

*S. Liu and S. K. Krueger
Department of Meteorology
University of Utah
Salt Lake City, Utah*

Introduction

Altocumulus (Ac) clouds are predominately water clouds and typically less than several hundred meters thick. Ac cloud heights are mid-level and tend to be from 2 km to 8 km. Because of their effects on solar and infrared radiation, Ac clouds play an important role in the earth's energy budget. Ac clouds are typically too thin to be vertically resolved in global climate models (GCMs). Fowler et al. (1996) indicate that the problem of subgrid-scale cloudiness has not yet been adequately addressed in climate models. The parameterization of the formation and structure of vertically subgrid-scale Ac layers has not been previously reported.

Last year, we reported on our development of an elevated mixed layer model (MLM) and the comparison of Ac layers simulated by the MLM and a cloud resolving model (CRM) for a period of 5 hr (Liu and Krueger 1998a, hereafter LK98a). This is a step toward incorporating a physically based parameterization for thin Ac layers into a GCM. The results from the MLM were in good or reasonable agreement with those from the CRM. Because a 5-hr time period is not long, we have since made a 20-hr comparison of simulated Ac layers from the CRM and MLM. In this report, we first introduce the CRM and the elevated MLM. Then, we compare liquid water path (LWP), cloud top, cloud base, and mixed layer base heights for the two models and present sensitivity tests for the MLM.

Description of Models

The CRM is based on the two-dimensional (2-D) (x - z) anelastic set of equations. It includes the hydrostatic, continuity, vorticity, thermodynamic, and total water equations. The CRM uses third-moment turbulence closure. The large eddies are explicitly represented, while the small-scale turbulence is parameterized with the turbulence closure. The CRM also includes a turbulence-scale condensation scheme, a bulk microphysics parameterization, and an advanced radiative transfer code. Neither the

ice-phase nor precipitation is considered in this study. The CRM is more fully described in Krueger (1988), Xu and Krueger (1991), and Krueger et al. (1995a, b).

The MLM is completely described in Liu and Krueger (1998b) and Liu (1998). It includes the prognostic equations for elevated Ac mixed-layer moist static energy, total water mixing ratio, top height z_T , and base height z_B . To close the MLM, the entrainment velocities must be parameterized based on assumptions about the turbulent structure of the mixed layer. We use a closure that is based on the entrainment parameterization of Turton and Nicholls (TN 1987). The entrainment velocity at the mixed layer top is

$$w_{eT} = \frac{A}{(z_T - z_B)\Delta s_{vT}} \int_{z_B}^{z_T} \overline{w's'_v} dz$$

where s_v is the virtual dry static energy, Δs_{vT} is the jump in s_v across the above-cloud inversion layer, and $\overline{w's'_v}$ is the vertical turbulent flux of s_v . We set the constant $A = 2.5$. We do not directly determine w_{eB} . Instead, we use TN's constraint on the buoyancy integral ratio (BIR):

$$\text{BIR} \equiv -\frac{\int_{z_B}^{z_C} \overline{w's'_v} dz}{\int_{z_C}^{z_T} \overline{w's'_v} dz} \leq \text{BIR}_{\max},$$

where z_c is the height of the cloud base and BIR_{\max} is a negative constant representing the maximum allowable turbulent kinetic energy loss due to buoyant consumption in the subcloud layer. As the mixed-layer top rises because of entrainment, z_B must typically also rise to prevent BIR from exceeding BIR_{\max} .

Simulations and Results

The initial profiles of potential temperature and water vapor mixing ratio for the CRM simulation are similar to those for

the thin cloud in LK98a. But the supersaturation region is lower, from 5.45 km to 5.65 km. The model domain is 3.2 km long and 8.9 km high. The horizontal grid interval is 50 m, while the vertical grid is 1 km from surface to 4 km, 500 m from 4 km to 4.5 km, and 25 m from 4.5 km to 7.9 km. The time step is 2.5 seconds. The total simulation time for the CRM is 36 hours.

In LK98a, there is an evident difference in LWP between the CRM and MLM 5-hr simulations. One of the reasons for this difference may be the initial conditions. In the 36-hr CRM simulation, the LWP is stable after 6 hr, so we use the CRM conditions at hour 6 to build the initial profiles for a MLM simulation. Also, the simulation time is only 5 hr for the previous MLM and CRM comparison. It is interesting to compare longer simulations.

The lower and upper boundaries of the mixed layer in the CRM simulations are determined by assuming that the turbulent kinetic energy (TKE) in the mixed layer is greater than $0.2 \text{ m}^2 \text{ s}^{-2}$. The upper boundary so determined coincides with the level where the cloud fraction equals 0.1. The moist static energy and total water mixing ratio at the inversion top (assumed to be 50 m above the mixed-layer top) are

$$h_{T+} \text{ (J/kg)} = 2.94801z + 293409,$$

$$q_{wT+} \text{ (g/kg)} = -1.33852 \times 10^{-4}z + 1.49565$$

where z is the height in meters. Other conditions are the same as in LK98a.

In Figure 1, the temporal behavior of the LWP is illustrated for these longer CRM and MLM simulations. The LWP for the MLM is smaller than that for the CRM from the starting time to hour 12. After this period, it becomes larger than that for the CRM. The largest difference is less than 20%. The agreement between the two models is fairly good for the LWP.

The temporal behavior of cloud top, cloud base, and mixed-layer base heights for the same CRM and MLM simulations is illustrated in Figure 2. We only compare these for the time period of the MLM simulation. The MLM cloud top ascends slightly more slowly than does the CRM cloud top, as does the MLM cloud base. The cloud top, cloud base, and ML base height for the two models agree quite well.

We compare the entrainment velocity at the ML top (w_{eT}) and detrainment velocity at the ML base (w_{eB}) for the two models. The range of w_{eT} for the MLM is small, from 1.15 cm s^{-1} to 1.52 cm s^{-1} , and the average is 1.21 cm s^{-1} . The average detrainment velocity at the lower boundary

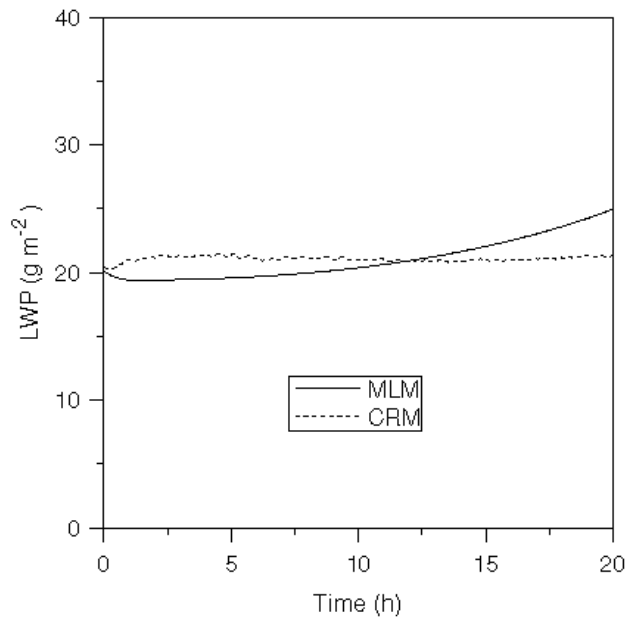


Figure 1. Evolution of the LWP for the CRM and MLM simulations.

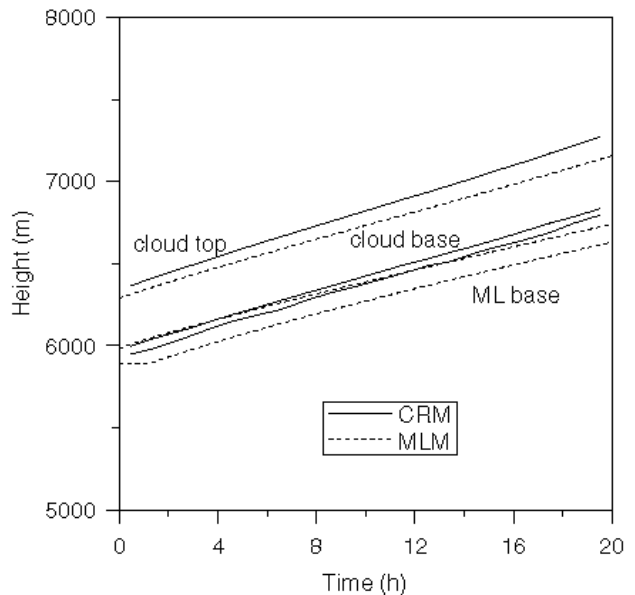


Figure 2. Evolution of cloud top, cloud base, and mixed-layer base heights for the CRM and MLM simulations.

(w_{eB}) for the MLM is 1.03 cm s^{-1} . The average w_{eT} and w_{eB} for the CRM during the same 20 hours are 1.35 cm s^{-1} and 1.25 cm s^{-1} , respectively. They are a bit larger than those for the MLM.

We also performed sensitivity tests for the MLM simulation. The temporal behaviors of cloud top, cloud base, and mixed-layer base heights and LWP for various values of the decoupling parameter BIR_{max} are shown in Figures 3 and 4, respectively. The BIR_{max} values used are the standard value, and half and double the standard value. The cloud top height is not sensitive to these changes until after hour 8. Then cloud top becomes higher for larger BIR_{max} . The cloud base height changes little when BIR_{max} is halved, but decreases when BIR_{max} is doubled. The cloud depth is therefore larger with larger BIR_{max} . The subcloud layer depth is also larger when BIR_{max} is larger. This occurs because BIR can be larger for larger BIR_{max} . The LWP is sensitive to BIR_{max} , and increases quickly when BIR_{max} is doubled; and decreases at first, then is stable when BIR_{max} is halved.

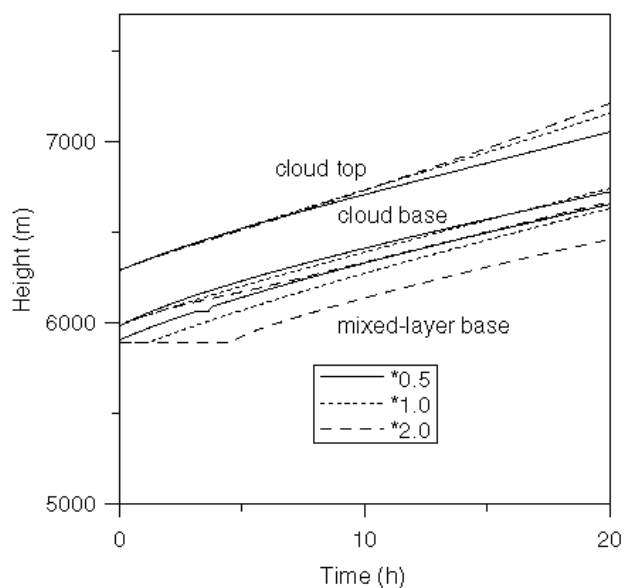


Figure 3. Evolution of cloud top, cloud base, and mixed-layer base heights for different BIR_{max} values: 0.5 \times , 1 \times , and 2 \times the standard value.

Figures 5 and 6 illustrate the effects of using a different value of A in the formula for w_{eT} . The cloud top height is not sensitive to A . The cloud base height is lower when A is larger. The cloud depth is therefore larger when A is smaller. The subcloud layer depth is also larger when A is smaller. The LWP is increased when A is decreased. The differences in LWP are large. The LWP is sensitive to A .

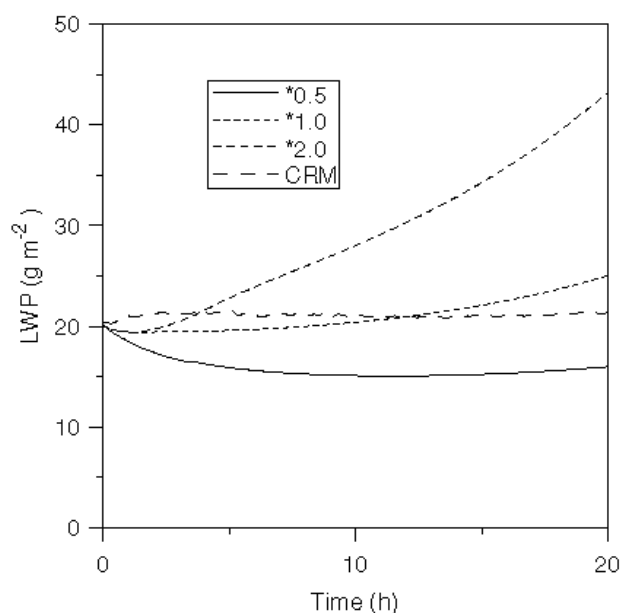


Figure 4. Evolution of the LWP for different BIR_{max} values: 0.5 \times , 1 \times , and 2 \times the standard value.

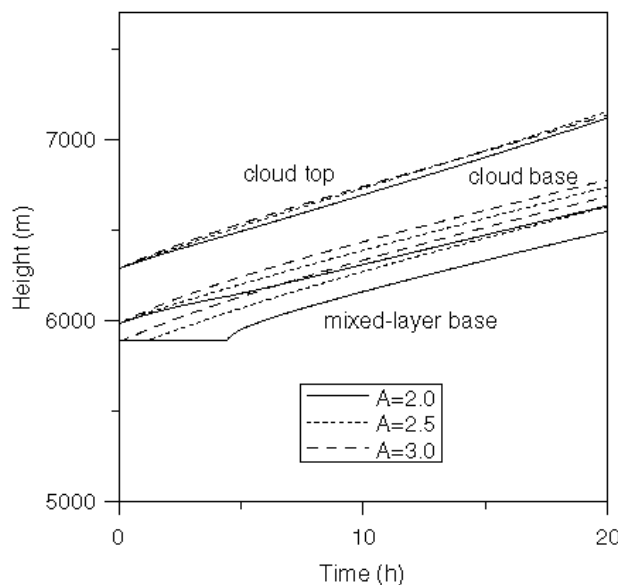


Figure 5. Evolution of cloud top, cloud base, and mixed-layer base heights for different values of the constant A .

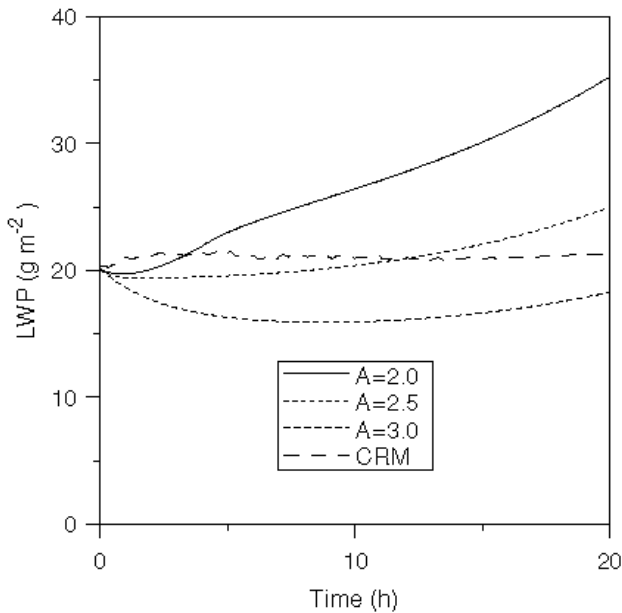


Figure 6. Evolution of the LWP for different values of the constant A.

Figures 7 and 8 illustrate the effects of using different above-cloud inversion layer depths (0 m, 50 m, and 100 m) in the MLM. The cloud top, cloud base, and mixed-layer base heights are not very sensitive to the inversion layer depth. In a study of a stratocumulus layer using a MLM, Siems et al. (1993) had a similar result. In their study, cloud top and base heights are similar for inversion layer depths equal to 0 m and 50 m. Figure 8 shows that the LWP is sensitive to the inversion depth, and is larger when the inversion depth is smaller. The associated small changes in cloud depth produce large changes in LWP.

Summary

A comparison between MLM and CRM simulations was made during a 20-hr period. The MLM results generally agreed with the CRM results for the LWP and the tendencies of the cloud top, cloud base, and mixed-layer base heights. Sensitivity tests show that w_{eT} and w_{eB} in the MLM depend on the constants A and BIR_{max} . The LWP in the MLM is also sensitive to changes in A, BIR_{max} , and the above-cloud inversion layer thickness. The cloud thickness is not strongly sensitive to changes in these constants, especially the above-cloud inversion layer thickness.

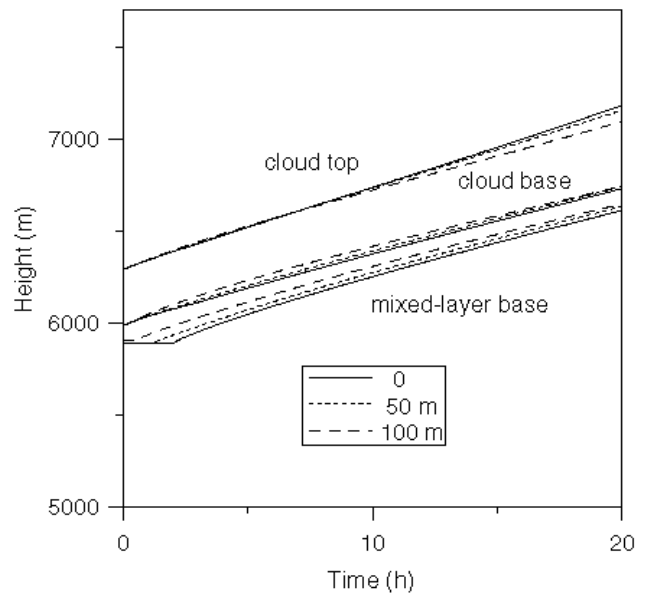


Figure 7. Evolution of cloud top, cloud base, and mixed-layer base heights for different above-cloud inversion layer depths.

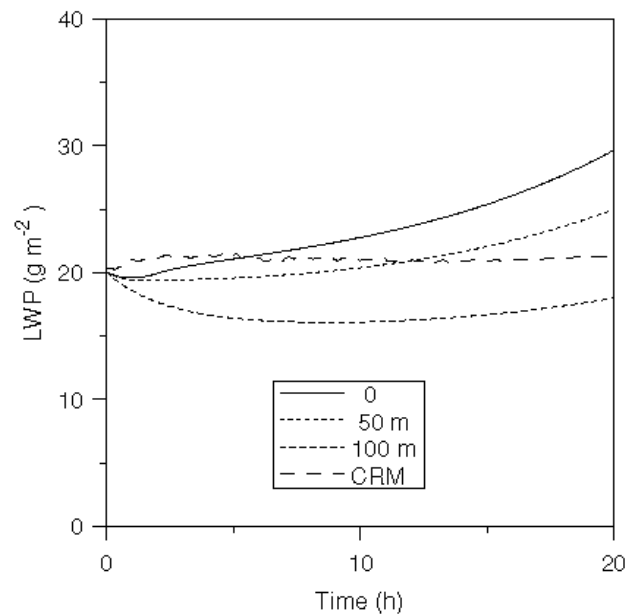


Figure 8. Evolution of the LWP for different above-cloud inversion layer depths.

Acknowledgments

This research was supported by the Environmental Science Division, U.S. Department of Energy (DOE), under Grant DE-FG03-94ER61769 and by the National Science Foundation (NSF) under Grant ATM 89-14348. Computing assistance was provided by National Center for Atmospheric Research (NCAR) SCD.

References

- Fowler, L. D., D. A. Randall, and S. A. Rutledge, 1996: Liquid and ice cloud microphysics in the CSU general circulation model. Part I: Model description and results of a baseline simulation. *J. Climate*, **9**, 489-529.
- Krueger, S. K., 1988: Numerical simulation of tropical cumulus clouds and their interaction with the subcloud layer. *J. Atmos. Sci.*, **45**, 2221-2250.
- Krueger, S. K., G. T. McLean, and Q. Fu, 1995a: Numerical simulation of the stratus to cumulus transition in the subtropical marine boundary layer. Part I: Boundary layer structure. *J. Atmos. Sci.*, **52**, 2839-2850.
- Krueger, S. K., G. T. McLean, and Q. Fu, 1995b: Numerical simulation of the stratus to cumulus transition in the subtropical marine boundary layer. Part II: Boundary layer circulation. *J. Atmos. Sci.*, **52**, 2851-2868.
- Liu, S., 1998: Numerical modeling of altocumulus cloud layers. Ph.D. dissertation, Department of Meteorology, University of Utah, 149 pp.
- Liu, S., and S. K. Krueger, 1998a: Development of an elevated mixed layer model for parameterizing altocumulus cloud layers. In *Proceedings of the Seventh Atmospheric Radiation Measurement (ARM) Science Team Meeting*, CONF-970365, pp. 227-231. U.S. Department of Energy.
- Liu, S., and S. K. Krueger, 1998b: Numerical simulations of altocumulus using a cloud resolving model and a mixed layer model. *Atmos. Res.*, **47-48**, 461-474.
- Siems, S. T., D. H. Lenschow, and C. S. Bretherton, 1993: A numerical study of the interaction between stratocumulus and the air overlying it. *J. Atmos. Sci.*, **50**, 3663-3676.
- Turton, J. D., and S. Nicholls, 1987: A study of the diurnal variation of stratocumulus using a multiple mixed layer model. *Quart. J. R. Met. Soc.*, **113**, 969-1009.
- Xu, K.-M., and S. K. Krueger, 1991: Evaluation of cloudiness parameterizations using a cumulus ensemble model. *Mon. Wea. Rev.*, **119**, 342-367.